

ECCC Developments in the Assessment of Creep-Rupture Properties

S R HOLDSWORTH[‡] & G MERCKLING[§]

[‡] ALSTOM Power, Rugby, UK

[§] Istituto Scientifico BREDA, Milan, Italy

INTRODUCTION

The European Creep Collaborative Committee (ECCC) is now in its third phase of activity since its formation in 1992.¹ First focussing on the provision of uniaxial rupture strength values for steels for European product and design standards (1992-6),² and then the assessment of weldments (1997-2001), the current emphasis for ECCC working groups is the analysis and application of creep deformation and ductility properties to the assessment of components and multi-axial features. The current initiative is referred to as *ADVANCED-CREEP* (2001-2005) and is supported by the European Commission Thematic Network contract GTC2-2000-33051.

ECCC was originally formed primarily to provide the means for European industry to combine its resources to influence the content of the wave of new European high temperature product and design standards in preparation during the early 1990s. Initially, the principal aims of ECCC were:

- to co-ordinate the generation of creep data throughout Europe,
- to interact with, and supply information to European standards organisations and their technical committees,
- to mutually exchange technical information relating to current and future activities on material developments, and
- to develop common rules for creep data generation, collation/exchange and assessment.

The defined objectives are being achieved through the efforts of a number of working groups whose activities are steered by the ECCC Management Committee (Fig. 1). The WG3x groups co-ordinate the main creep data generation (testing), collation and assessment activities directed towards influencing the content of European standards/codes (Fig. 2). The respective WG3x areas of responsibility are presently:

- WG3A: Low and high alloy ferritic steels
- WG3B: Low and high alloy austenitic steels
- WG3C: Nickel base alloys

Technical support is provided by WG1 and its sub-groups. The main role of WG1 is to provide recommendations on procedures for data generation, collation and assessment to form the basis of common practices followed within ECCC.³ These recommendations are published and are thereby available to other users. They are acknowledged to have influenced several important standards.⁴⁻⁶ Two WG1 sub-groups focus specifically on the provision of procedures relating to post service exposed materials (WG1.1) and creep crack initiation data (WG1.2), Fig. 1.

At the start of the *ADVANCED-CREEP* phase of activity, a new working group was formed to focus on the assessment of high temperature components and multi-axial features (i.e. WG4). When ECCC was first formed, its main activity was driven by the requirements of alloy producers and plant manufacturers. More recently, the requirements of plant operators have become increasingly important. This is reflected by the creation of WG1.1 in 1997 and in particular now by the formation of WG4 to provide support for plant design and assessment functions (as shown in Fig. 2).

The following paper focuses on the present activities of WG1. During the *ADVANCED-CREEP* initiative, the main concerns of this group are the analysis and application of creep deformation and ductility properties to the assessment of components and multi-axial features.

CREEP-RUPTURE DATA ASSESSMENT

ECCC developments relating to the assessment of stress-rupture data are well documented.^{3,7} Reference has already been made to the requirement during the 1990s for well-substantiated, European industry endorsed creep-rupture strength values for new European high temperature product and design standards. The basis for these was the largest possible acceptable dataset for material of a given specification, e.g. the X10CrMo9-10(a) SR dataset in Table 1. The ECCC Recommendation Volumes were created to provide guidance for the generation, collation and assessment of such datasets.³

Not least because of the large number of high temperature product standards in preparation at the time, it was necessary to share the workload and the required stress-rupture data assessments were performed by assessors from different countries, adopting various approaches. In order to ensure a level of consistency in the strength values determined in these circumstances, WG1 developed a philosophy which restricted the number of assessment procedures used to those which were well defined and which had been validated in an extensive assessment inter-comparison activity involving the four large SR working datasets referred to in Table 1.^{3,7} Most importantly, the assessment results had to meet the acceptance criteria of a number of post assessment tests (PATs). The ECCC PATs are now widely accepted and form an integral part of modern creep-rupture data assessment procedures, e.g. PD6605, DESA.^{4,8}

Guidance is not restricted to the assessment of large stress rupture datasets, and now encompasses the assessment of smaller datasets,^{3,7} e.g. those for weldments.

CREEP STRAIN ANALYSIS

BACKGROUND

The current ECCC evaluation of creep strain analysis methods involves a review and evaluation of model equations in common use for representing creep deformation data and an assessment of their effectiveness for various materials and practical applications.

Creep strain $\epsilon_f(t)$ or $e_p(t)$ curves are determined from the results of continuous-measurement or interrupted tests involving the application of a constant load (or stress) to a uniaxial testpiece held at constant temperature (Fig. 3a). In continuous-measurement tests, the creep strain, ϵ_f , is monitored without interruption by means of an extensometer attached to the gauge length of the testpiece. In interrupted tests, the total plastic strain, e_p , is measured optically at room temperature during planned interruptions ($e_p = \epsilon_f + e_r$, Fig. 3b). A list of symbols and terms is given in the Nomenclature.

Depending on the nature of the creep model application, the analysis will be of several $\epsilon_f(t)$ or $e_p(t)$ curves determined for a single heat or several heats of the specified material. The creep strain curves may have been determined from a matrix of $t(T, \mathbf{s})$ tests for which T and \mathbf{s} are *i*) relatively homogeneously distributed or *ii*) inhomogeneously distributed. Case *i*) is the ideal situation and generally arises within R&D projects or from well co-ordinated data generation activities. Case *ii*) is more typical of large multi-national datasets gathered to produce creep strength values for standards.

During the first phase of ECCC activity, WG1 evaluated the applicability of post assessment tests to the results of $R_{pe/t/T}$ creep strength assessments.^{3e} Such evaluations do not necessarily involve individual $e_p(t)$ curve fitting, and typically entail large Case *ii*) type datasets (e.g. X10CrMo9-10(b), Table 1).⁹ The prescribed post assessment tests provided an effective tool for evaluating assessed creep strength acceptability in these circumstances. The focus of current WG1 activity is on creep strain assessment involving individual $e_p(t)$ curve fitting.

It is recognised that many different model equations are used to represent creep strain behaviour, ranging from simple-phenomenological to complex-constitutive. A number of model equations commonly used to represent creep strain development in engineering steels are listed in Appendix A. The listing is not exhaustive and simply reflects those expressions most commonly used by organisations currently active in ECCC. Similar creep model equation forms are grouped together in

Table 2. For example, the Garofalo, BJJ and Theta expressions (Eqns. A5-A9) share a similar representation of primary creep.

Certain expressions are likely to be better suited for specific materials and analytical applications. For example, the overall primary (P), secondary (S) and tertiary (T) creep strain characteristics of a particular steel (Fig. 3a) may not be acceptably modelled by certain creep equation forms. Moreover, some applications only require a knowledge of primary low strain creep behaviour whereas others need a representation of the full creep curve. One purpose of the present evaluation is to identify the respective suitability of commonly used creep equations (e.g. Table 2).

ASSESSMENT INTER-COMPARISON

The latest WG1 creep strain data assessment inter-comparison was based on a Case *i*) type single-heat, uniformly-distributed creep-rupture (CR) dataset for 10CrMo9-10 (*c*) in Table 1). The model equations applied by different assessors are evident in Table 2. For most of the analysis approaches adopted, it was first necessary to curve-fit individual $\epsilon_p(t)$ records, and this activity highlighted the importance of optimising the fitting procedure (e.g. by minimising residual errors). The way in which this is achieved can vary with model equation (and material). For example, good results for the Theta expression (Eqn. A8) could be obtained by independently minimising the errors during curve-fitting the primary/secondary and secondary/tertiary regimes of the X10CrMo9-10 $\epsilon_p(t)$ records.

The results of individual $\epsilon_p(t)$ curve-fits are combined to provide the master-equation parameters. The effectiveness of the respective master-equations to represent observed $\epsilon_p(t)$ behaviour was examined in the following way. Plastic strains of 0.2 and 1.0% were selected to represent typical low and high strain industrial requirements. For each assessment, plots of $\log(t_{pe/S/T}^*)$ versus $\log(t_{pe/S/T})$ for the two strain levels were constructed with reference to the following relationships (e.g. Fig. 4.):

$$\log(t_{pe/S/T}^*) = \log(t_{pe/S/T}) \pm \log(2) \quad (\text{dotted lines in Fig. 4}) \quad (1)$$

$$\log(t_{pe/S/T}^*) = \log(t_{pe/S/T}) \pm 2.5 \cdot s_{A-RLT} = \log(t_{pe/S/T}) \pm \log(Z) \quad (\text{chain lines in Fig. 4}) \quad (2)$$

where for a normal distribution, almost 99% of the observed times to specific strain values would be expected to lie within the boundary lines defined by Eqn. 2.

A perfect prediction of $t_{pe/S/T}$ by the master-equation is represented by Z equal to zero. Ideally Z is ≤ 2 , such that the chain lines in Fig. 4 fall on top of (or within) the dotted lines defined by Eqn. 1. Z values of >4 are unacceptable, whereas values of $\leq 3-4$ are marginal but may be regarded as practically acceptable. The Z values determined in the present inter-comparison are summarised in Table 2.

The effectiveness of the evaluated models to master-equation predict $t_{pe/S/T}$ varied with specific strain value for the 10CrMo9-10(*c*) dataset. For example, the Theta expression is most effective at predicting times to 1% strain and less so for times to 0.2% strain (Fig. 4). The modified-Garofalo model is particularly effective for predicting times to low and high strains according to this study (Table 2), although it should be acknowledged that the adopted analysis approach involved an intensive prior individual $\epsilon_p(t)$ curve fitting procedure. It is of little surprise that the Z values for the Omega model predictions of times to the selected strains were poor (Table 2) since this expression was developed to represent tertiary creep behaviour, i.e. $\epsilon_p > 1\%$.

Current assessment inter-comparison activity involves a larger Case *ii*) type multi-source, multi-heat, inhomogeneously-distributed CR dataset for X10CrMoVNb9-1 (Table 1). The heat-to-heat variability in Case *ii*) type datasets is typically such that the incorporation of a metallurgical characterising parameter into the model equation will be necessary to achieve the same Z values determined for the smaller Case *i*) type single heat, homogeneously distributed 10CrMo9-10(*c*) dataset.

RUPTURE DUCTILITY

Uniaxial rupture ductility can vary with stress (time) and temperature in a relatively complex way (e.g. Fig. 5). The various ductility regimes are associated with distinct rupture mechanisms. For example in ferritic steels, Regime-I involves ductile rupture resulting from the formation of voids typically as a consequence of particle/matrix decohesion. Regime-II is a transition region in which the ductility drops due to the increasing incidence of grain boundary cavitation, but still accompanied by relatively high levels of matrix deformation. In Regime-III, rupture is by the nucleation and subsequent diffusive growth of grain boundary cavities. In Regime-IV, overaging of the microstructure lowers the rate of cavity nucleation and/or growth leading to a progressive recovery of ductility. The mechanisms associated with the identified ductility regimes can differ for different alloy systems. The analytical representation of rupture ductility data has not previously received significant attention.

Rupture ductility data assessment comparisons are being conducted on the large stress-rupture working datasets employed previously by WG1^{3e,7} (i.e. for 10CrMo9-10(a), X19CrMoVNb11-1, X7CrNi18-9, and X5NiCrAlTi31-20, Table 1). The X19CrMoVNb11-1 dataset is of particular interest in that it exhibits the four ductility regimes shown in Fig. 5. Moreover, it is a large multi-source, multi-heat, multi-temperature data collation typical of those used for the determination of creep parameters for standards. The lower data bounds for each temperature are shown in Fig. 6. The added complexity due to the multi-heat nature of this dataset is evident in Fig. 7.

Initial assessments were performed using the Spindler model, developed to model grain boundary cavity nucleation and growth processes.²¹ The form of Eqn. B1 (and all other rupture ductility model equations in Appendix B) is adopted to enable a maximum upper-shelf ductility to be set, which may simply be a temperature dependent tensile ductility function. The Spindler model was specifically developed to relate fracture elongation to strain rate for the determination of creep damage due to secondary loading in terms of ductility exhaustion, e.g. for the assessment of creep-fatigue damage.

The ability of the Spindler model to predict mean rupture ductility with respect to time for the X19CrMoVNb11-1 dataset is shown in Fig. 7. A target requirement from $A_u(t)$ assessments is the description of minimum rupture ductility as a function of stress and temperature to long times. The example provided by Fig. 7 demonstrates the need for including a metallurgical characterising function in the model form, in particular for the assessment of large inhomogeneously distributed multi-heat datasets.

The applicability of several simple phenomenological expressions to characterise the large datasets is also being evaluated, i.e. Eqns. B2-B4. An example of the effectiveness of an equation form based on the Soviet model²² to predict the mean rupture ductility characteristics of X5NiCrAlTi31-20 is shown in Fig. 8. A fundamental problem with the analytical prediction of rupture ductility as a function of time is that both parameters are response variables dependent on temperature and stress. The rigorous analytical treatment of rupture ductility behaviour is a challenge which will occupy the resources of WG1 for the remainder of the *ADVANCED-CREEP* work programme.

CONCLUDING REMARKS

ECCC developments in the assessment of creep-rupture properties have been reviewed with particular emphasis on current activities.

A significant effort is being devoted to the formulation of recommendations concerning the assessment of creep strain. There are several model equations available for characterising the primary, secondary and tertiary creep deformation characteristics, ranging in complexity from simple-phenomenological to full-constitutive. The suitability of some of these to specific material classes and analytical applications is reviewed.

In those creep strain assessment procedures involving prior individual $\epsilon(t)$ curve-fitting, best results are obtained by optimising the procedure adopted to fit specific model equations to the deformation characteristics of specific material types.

A method of qualifying the effectiveness of a creep strain equation for specific material types and analytical applications is introduced.

In most assessments of creep strain characteristics from large, multi-source, multi-heat, multi-temperature datasets, the adoption of a heat-by-heat analysis procedure will be necessary.

The assessment of creep-ductility is complicated by the fact that the data can represent rupture characteristics in up to four different mechanism regimes at main high-temperature material application temperatures. The analytical representation of rupture ductility data has not previously received significant attention.

The rigorous analytical description of rupture ductility as a function of time (a second response variable dependent on temperature and stress) is providing a significant ongoing challenge.

In the meantime, the ability of a number of model equations to simply represent the mean rupture characteristics of large datasets of low and high alloy ferritic and austenitic steels is being evaluated. A current development is the incorporation of a metallurgical characterising function into selected model forms as an integral part of defining minimum rupture behaviour, in particular for the assessment of large inhomogeneously distributed multi-heat datasets.

ACKNOWLEDGEMENTS

The authors acknowledge the significant contribution of past and present members of ECCC-WG1 and, specifically to Dr M Askins (Innogy), Prof. E Gariboldi (Politecnico-Milano), Dr P Morris (Corus), Dr S Spigarelli (Univ.Ancona), Dr M Spindler (British Energy) and Dr M Schwienheer (IfW-TUD) for assessment activity referred to in the present paper.

They would also like to acknowledge the support of the EC through the *ADVANCED-CREEP* Thematic Network contract GTC2-2000-33051, and to the co-ordination and secretariat support provided by ETD.

REFERENCES

- 1 D.V. Thornton, 'Activities of the European Creep Collaborative Committee', *Proc. 5th Intern. Parsons Conf. on Advanced Materials for 21st Century Turbines and Power Plant, Cambridge*, 3-7/7/00, A. Strang et al. eds., IOM London, 2000, 123-128.
- 2 ECCC Data Sheets, 'Rupture strength, creep strength and relaxation strength values for carbon-manganese, low alloy ferritic, high alloy ferritic and austenitic steels, and high temperature bolting steels/alloys', D.G. Robertson ed., ERA Technology publ., 1999.
- 3 ECCC Recommendations, 'Creep data validation and assessment procedures', S.R. Holdsworth et al. eds., ERA Technology publ., 2001, (a) Vol.1: Overview, (b) Vol.2: Terms and terminology, (c) Vol.3: Data acceptability criteria, Data generation, (d) Vol.4: Data exchange and collation, (e) Vol.5: Data assessment.
- 4 BS PD6605, *Guidance on Methodology for the Assessment of Stress-Rupture Data*, British Standards Institution, 1998.
- 5 EN 10291, *Metallic Materials, Uniaxial Creep Testing in Tension, Method of Test*, European Norm, 2000.
- 6 prEN 10319, *Metallic Materials, Tensile Stress Relaxation Testing*, European Norm, provisional, 2000.
- 7 S.R. Holdsworth, 'Recent developments in the assessment of creep-rupture data', *Proc. 8th Intern. Conf. on Creep and Fracture of Engineering Materials and Structures*, Tsukuba, 1-4/11/99, JSME, 1999, 1-8.
- 8 J. Granacher & M. Monsees, 'Assessment procedure document for DESA', *Appendix D2 in ECCC Recommendations Vol.5*,^{3e} 1996.
- 9 C.K. Bullough & S.R. Holdsworth, 'New strategies for the assessment of long-term data from interrupted creep tests', *Proc. 3rd Intern. Conf. on Engineering Structural Integrity: Life Assessment and Life Extension of Engineering Plant, Structures and Components*, Cambridge, AEA, 24-26/9/1996.
- 10 F.H. Norton, *The Creep of Steel at High Temperature*, McGraw-Hill, 1929.

- 11 H. Bartsch, 'A new creep equation for ferritic and martensitic steels' *Steel Research*, 1995, **66** (9), 384-388.
- 12 F. Garofalo, *Fundamentals of Creep and Creep Rupture in Metals*, MacMillan, New York, 1965.
- 13 J. Granacher, H. Möhlig, M. Schwienheer & C. Berger, 'Creep equation for high temperature materials', *Proc. 7th Intern. Conf. on Creep and Fatigue at Elevated Temperatures (Creep 7)*, 3-8/6/01, NIRM, Tsukuba, 2001, 609-616.
- 14 D.I.G. Jones, D.L. Bagley, 'A renewal theory of high temperature creep and inelasticity', *Proc. Conf. on Creep and Fracture: Design and Life Assessment at High Temperature*, London, 15-17/4/96, MEP, 1996, 81-90.
- 15 R.W. Evans & B. Wilshire, *Creep of Metals and Alloys*, Inst. Metals, 1985.
- 16 L.M. Kachanov, *Introduction to Continuum Damage Mechanics*, Martinus Nijhoff Publ., 1986.
- 17 B.F. Dyson & M. McClean, 'Microstructural evolution and its effects on the creep performance of high temperature alloys', *Microstructural Stability of Creep Resistant Alloys for High Temperature Applications*, A. Strang et al. eds., 1998, 371-393.
- 18 Creep of Steels Working Party, *High Temperature Design Data for Ferritic Pressure Vessel Steels*, Inst. Mech.Eng., London, 1983.
- 19 J. Bolton, 'Design considerations for high temperature bolting', *Proc. Conf. on Performance of Bolting Materials in High Temperature Plant Applications*, York, 16-17/6/94, A Strang ed., 1994, 1-14.
- 20 M. Prager, 'Development of the MPC Omega method for life assessment in the creep range', *ASME J. Pressure Vessel Technology*, 1995, **117**, May, 95-103.
- 21 M.W. Spindler, 'The multi-axial creep ductility of austenitic stainless steel', *Fat. & Fract. of Engng. Mat. & Struct.*, 2003, submitted for publication.
- 22 I.I. Trunin, N.G. Golobova & E.A. Loginov, 'New method of extrapolation of creep test and long time strength results', *Proc. 4th Int. Symp. on Heat Resistant Metallic Materials*, Mala Fatra, CSSR, 1971, 168.

NOMENCLATURE

Several lower case symbols with subscripts are not specifically defined, but are constants associated with the creep strain and ductility equations given in the appendices.

A, A_u	tensile elongation, elongation at rupture
CR	creep-rupture test
E, E_T	elastic modulus, elastic modulus at temperature
ECCC	European Creep Collaborative Committee
m_s, m_l	exponents in Spindler equation (B1)
n	stress exponent
$N_{\text{heats}}, N_{\text{tests}}, N_T$	number of heats, number of tests, number of temperatures
p	time exponent
P	primary (creep regime)
PATs	post assessment tests
Q	activation energy for creep
R	universal gas constant
$R_{pe/t/T}, R_{u/t/T}$	creep strength and rupture strength for a given time and temperature
$s_{A\text{-RLT}}$	standard deviation of residual log times
S	secondary (creep regime)
SR	stress rupture test
t	time
$t_u, t_{u,\text{max}}$	observed time to rupture, maximum observed time to rupture
t_{tot}	sum of testing times in a given dataset
$t_{pe/s/T}, t_{pe/s/T}^*$	observed and predicted times to given plastic strain
T	temperature
T	tertiary (creep regime)

Z	factor quantifying effectiveness of master creep equation to predict times to specific strains (see Eqn. 2)
\mathbf{e} , \mathbf{e}_e , \mathbf{e}_i	strain, elastic strain, instantaneous plastic strain
\mathbf{e}_f , \mathbf{e}_p , \mathbf{e}_{per}	creep strain, plastic strain, permanent strain
$\dot{\mathbf{e}}$, $\dot{\mathbf{e}}_{f,min}$, $\dot{\mathbf{e}}_{ave}$	strain rate, minimum creep strain rate, average strain rate
\mathbf{s} , \mathbf{s}_o	stress, initial stress
q_1 , q_2 , q_3 , q_4	constants in Theta equation (A8)
q_m	additional constant in modified Theta equation (A9)
Ω	material creep damage susceptibility parameter
w , \dot{w}	damage, rate of damage accumulation

Table 1 Summary statistics of WG1 working datasets

MATERIAL	DATASET TYPE	N_{tests}	N_{heats}	N_T	$t_{u,max}$ kh	t_{tot} kh
10CrMo9-10(a)	SR	1017	98	9	141	16,607
10CrMo9-10(b)	CR	217	8	6	199	4,060
10CrMo9-10(c)	CR	30	1	5	3	19
X10CrMoVNB9-1	CR	90	6	13	50	842
X19CrMoVNB11-1	SR	360	18	5	128	8,147
X2CrNi18-9	SR	843	96	24	111	7,549
X5NiCrAlTi31-20	SR	552	33	12	79	7,153

CR is creep-rupture, SR is stress-rupture

Table 2 Range of application of some creep equations with summary of results of 10CrMo9-10(c) creep strain data assessment inter-comparison

MODEL EQUATION	REF	RANGE OF APPLICATION		Z (10CrMo9-10)	
		REGIME	MATERIALS	$t_{0.2\%/S/T}$	$t_{1.0\%/S/T}$
Norton ¹⁰	A1	S	low/high alloy ferritic & austenitic steels, Ni base alloys, non-ferrous alloys		
Mod-Norton	A2	S	Ni-base alloys		
Norton-Bailey	A3	P/S	low/high alloy ferritic & austenitic steels		
Bartsch ¹¹	A4	P/S	low/high alloy ferritic, austenitic steels	3	4
Garofalo ¹²	A5	P/S	low/high alloy ferritic & austenitic steels, Ni base alloys, non-ferrous alloys		
Mod-Garofalo ¹³	A6	P/S/T	low/high alloy ferritic steels, Ni base alloys	2	2
BJF ¹⁴	A7	P/S	high alloy ferritic steels	15	4
Theta ¹⁵	A8	P/S/T	low/high alloy ferritic & austenitic steels, Ni-base alloys, non-ferrous alloys	17	2
Mod-Theta	A9	P/S/T	low/high alloy ferritic, austenitic steels, Al alloys, Al-matrix composites	10	4
Rabotnov-Kachanov ¹⁶	A10	P/S/T	low alloy ferritic steels		
Dyson & McLean ¹⁷	A11	P/S/T	low alloy ferritic steels, Ni-base alloys	12	3
I.Mech.E ¹⁸	A12	P/S	CMn, low/high alloy ferritic & austenitic steels		
Bolton ¹⁹	A13	P/S/T	low/high alloy ferritic & austenitic steels	4	13
Omega ²⁰	A14	S/T	low/high alloy ferritic steels	468	10

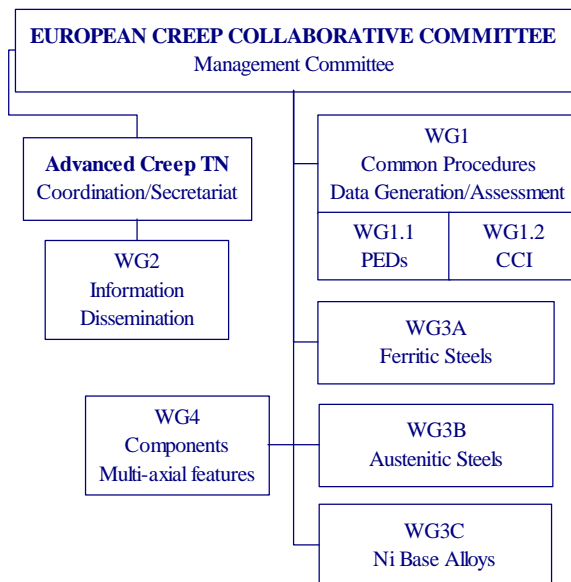


Fig. 1 Current structure of European Creep Collaborative Committee (ECCC)

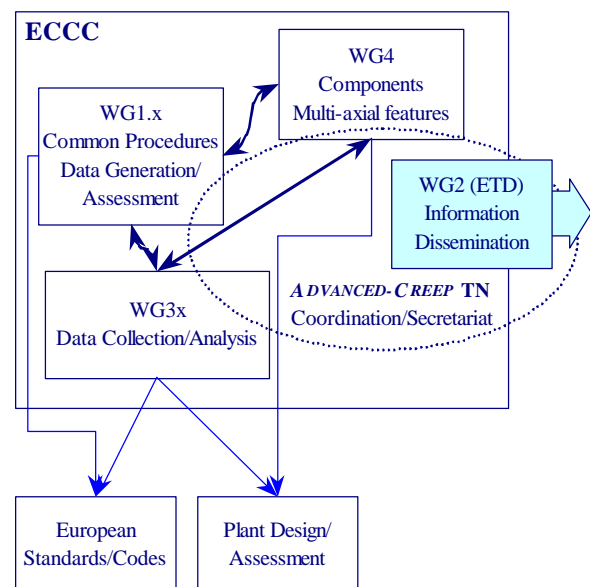


Fig. 2 Relationship between ECCC, the *ADVANCED-CREEP* TN and external organisations

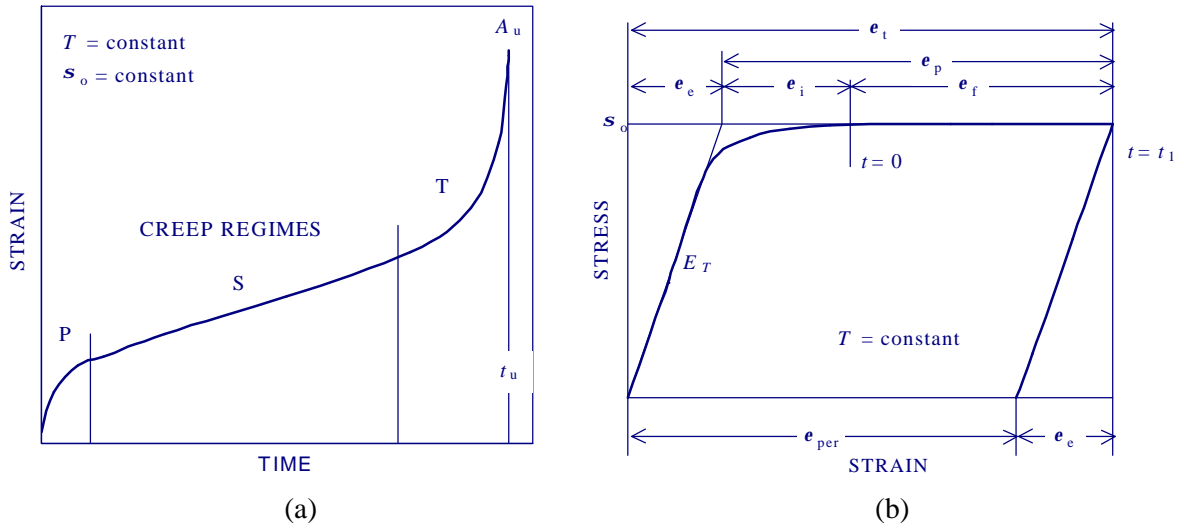


Fig. 3 Schematic diagrams showing (a) primary, secondary and tertiary creep regimes, and (b) strains generated during loading of creep test

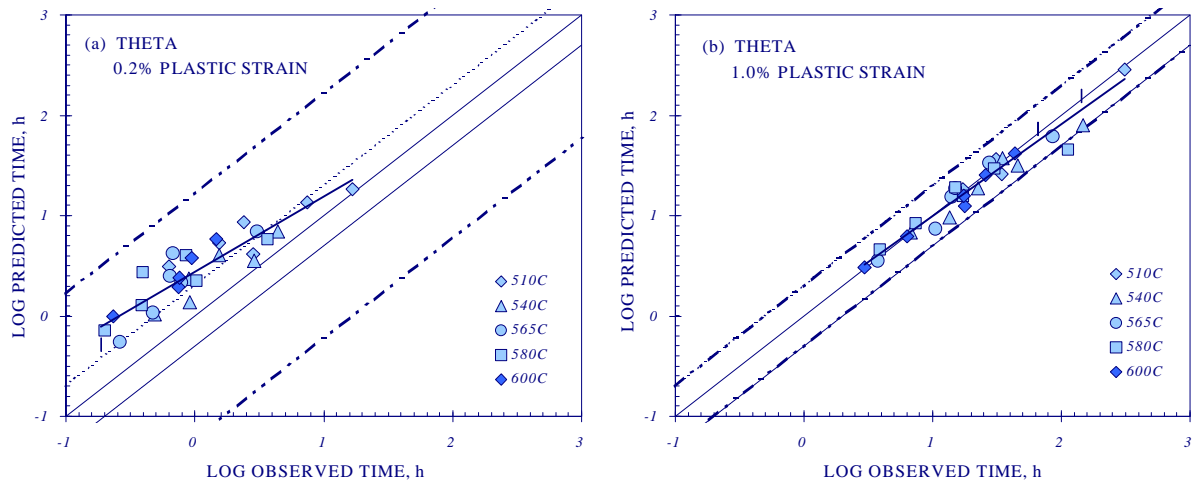


Fig. 4 Example comparisons of predicted and observed times to 0.2% and 1.0% plastic strain for the Theta creep equations in the assessment inter-comparison (see text for key to reference lines)

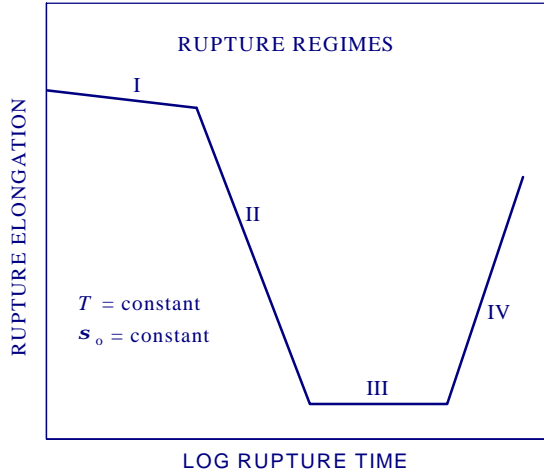


Fig. 5 Schematic representation of regimes of rupture ductility

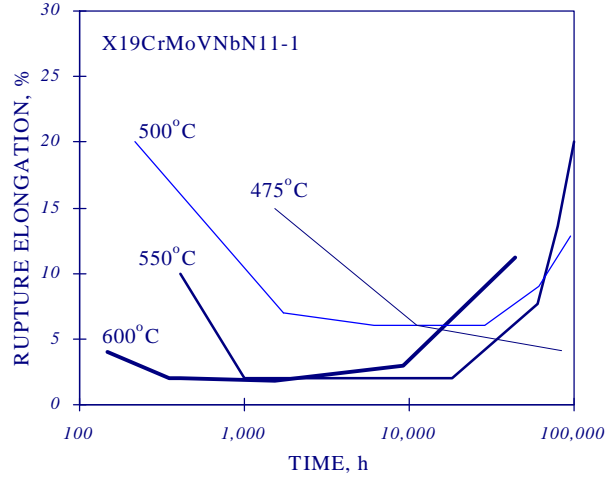


Fig. 6 Minimum $A_u(T)$ rupture elongation profiles for X19CrMoVNbN11-1 steel

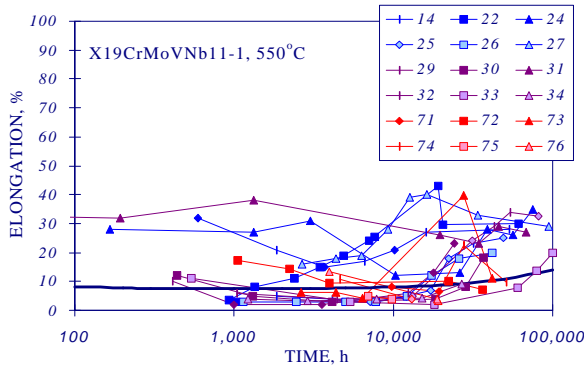


Fig. 7 Comparison of Spindler model equation fit (B1, solid line) with X19CrMoVNb11-1 rupture elongation data at 550°C

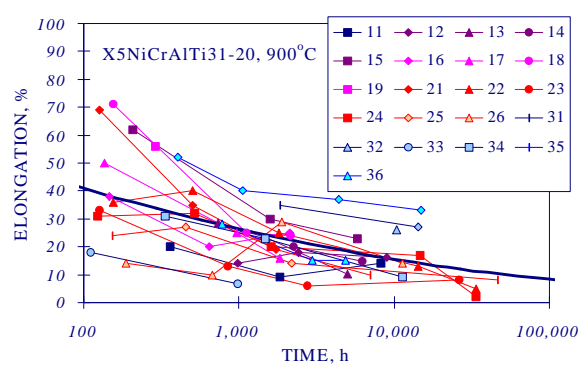


Fig. 8 Comparison of Soviet model equation fit (B4, solid line) with X5NiCrAlTi31-20 rupture elongation data at 900°C

APPENDIX A

CREEP STRAIN EQUATIONS

A1 Norton¹⁰

$$\dot{\epsilon}_{f,\min} = a_1 \cdot \exp(Q/RT) \cdot s^n$$

A2 Modified Norton

$$\dot{\epsilon}_{f,\min} = b_1 \cdot \exp(Q_B/RT) \cdot s^n + c_1 \cdot \exp(Q_C/RT) \cdot s^n$$

A3 Norton-Bailey

$$e_f = d_1 \cdot s^n \cdot t^p$$

A4 Bartsch¹¹

$$e_f = e_1 \cdot \exp(Q_1/RT) \cdot s \cdot \exp(b_1 \cdot s) \cdot t^p + e_2 \cdot \exp(Q_2/RT) \cdot s \cdot \exp(b_2 \cdot s) \cdot t$$

A5 Garofalo¹²

$$e_f = e_t \cdot [1 - \exp(-b_1 \cdot t)] + \dot{\epsilon}_{f,\min} \cdot t$$

- A6 Modified Garofalo¹³ $\mathbf{e}_f = \mathbf{e}_{f1} \left[1 - \exp\left(-g_1 \cdot (t/t_{12})^u\right) + \dot{\mathbf{e}}_{f,\min} \cdot t + c_{23} \cdot (t/t_{23})^f \right]$
- A7 BJF¹⁴ $\mathbf{e}_f = n_1 \cdot [1 - \exp(-t)]^b + n_2 \cdot \underline{t}$ where $\underline{t} = (\mathbf{s}/A_1)^n \cdot \exp(-Q/R.T)$
- A8 Theta¹⁵ $\mathbf{e}_f = \mathbf{q}_1 \cdot [1 - \exp(-\mathbf{q}_2 \cdot t)] + \mathbf{q}_3 \cdot [\exp(\mathbf{q}_4 \cdot t) - 1]$
where $\log(\mathbf{q}_i) = a_i + b_i \cdot T + c_i \cdot \mathbf{s} + d_i \cdot \mathbf{s} \cdot T$
- A9 Modified Theta $\mathbf{e}_f = \mathbf{q}_1 \cdot [1 - \exp(-\mathbf{q}_2 \cdot t)] + \mathbf{q}_m \cdot t + \mathbf{q}_3 \cdot [\exp(\mathbf{q}_4 \cdot t) - 1]$
where $\mathbf{q}_m = A \cdot \mathbf{s}^n \cdot \exp(-Q/R.T)$
- A10 Rabotnov-Kachanov¹⁶ $\dot{\mathbf{e}} = \frac{h_1 \cdot \mathbf{s}^n}{(1 - \mathbf{w})}$ $\dot{\mathbf{w}} = \frac{k_1 \cdot \mathbf{s}^n}{(1 - \mathbf{w})^z}$
- A11 Dyson & McClean¹⁷ $\dot{\mathbf{e}}_f = \dot{\mathbf{e}}'_o \cdot (1 + D_d) \cdot \exp(Q/R.T) \cdot \sinh\left(\frac{\mathbf{s} \cdot (1 - H)}{\mathbf{s}_o \cdot (1 - D_p) \cdot (1 - \mathbf{w})}\right)$
- A12 IMechE¹⁸ $R_{u/t/T} = (a_1 + b_1/\mathbf{e} - c_1 \cdot \mathbf{e}^2) \cdot R_{e/t/T} + d_1 + e_1/\mathbf{e} + f_1/\mathbf{e}^2 - g_1 \cdot \mathbf{e}^2$
- A13 Bolton¹⁹ $\mathbf{e}_f(\mathbf{s}) = \mathbf{e} \cdot (R_{u/t/T} / R_{e/t/T} - 1) / (R_{u/t/T} / \mathbf{s} - 1)$
- A13 Omega²⁰ $\dot{\mathbf{e}}_f = \dot{\mathbf{e}}_{f,\min} / (1 - \dot{\mathbf{e}}_{f,\min} \cdot \Omega \cdot t)$

APPENDIX B

RUPTURE DUCTILITY EQUATIONS

- B1 Spindler²¹ $\ln(A_u) = \text{MIN} \left| \left[\ln(A_1) + \frac{\Delta Q}{R.T} + n_1 \cdot \ln(\dot{\mathbf{e}}_{av}) + m_1 \cdot \ln(\mathbf{s}) \right], \ln(A(t)) \right|$
- B2 Evans & Wilshire¹⁵ $\ln(A_u) = \text{MIN} | [a_1 + b_1 \cdot \mathbf{s} + c_1 \cdot T + d_1 \cdot \mathbf{s} \cdot T], \ln(A(t)) |$
- B3 Anon $\ln(A_u) = \text{MIN} | [a_1 + b_1 \cdot \ln(\mathbf{s}) + c_1/T + d_1 \cdot \ln(\mathbf{s})/T], \ln(A(t)) |$
- B4 Soviet Model²² $\ln(A_u) = \text{MIN} | [a_1 + b_1 \cdot \log(T) + c_1 \cdot \log(\mathbf{s}) + d_1/T + e_1 \cdot \mathbf{s}/T], \ln(A(t)) |$